Accurate Localization and Tracking of a Passive RFID Reader Based on RSSI Measurements

Saurav Subedi, Eric Pauls, and Yimin D. Zhang

***Abstract*—Real-time locating systems require high localization accuracy in the order of a few centimeters. Conventional methods for radio frequency identification (RFID) localization fail to achieve such accuracy, particularly in complex radio frequency propagation environments. In this paper, we propose a method for locating and tracking an RFID reader that can achieve such accuracy in a complex propagation environment by exploiting received signal strength indicator (RSSI) measurements as the only form of observation obtained from multiple spatially distributed passive tags. There are three key contributions of this work. First, we analyze the effect of propagation impairments, non-isotropic radiation pattern of the tag antennas and multipath propagation, on RSSI measurements and the overall localization and tracking performance. Next, we compensate for the artifacts of multipath propagation and non-isotropic antenna pattern and obtain a maximum likelihood (ML) estimate of the RFID reader in a two-dimensional Cartesian space. The ML estimates of the reader position, together with its velocity, are then used as inputs to the Kalman filter for dynamical estimation of its trajectory. Finally, we present experimental results to demonstrate that the proposed method substantially improves the localization accuracy compared to other state-of-the-art methods for a given tag density.**

***Index Terms*—Passive RFID, localization, tracking, multilateration, RSSI, multipath propagation, antenna pattern.**

I. INTRODUCTION

RADIO frequency identification (RFID) is an important technology for a diverse range of applications involving electronic identification, localization, and tracking [1–3]. With the advent of real-time locating systems applications, research efforts have concentrated on improving the accuracy of location estimation algorithms [4–7]. As such, in the context of several current and emerging applications, such as telemedicine [8] and gesture recognition [9], accuracy of localization has emerged as a key challenging issue in RFID localization and tracking systems.

Typically, localization of an RFID-enabled object is implemented as a two-step process [2]. First, the range and/or direction-of-arrival (DOA) information of the object is estimated from the observed RFID signal. The DOA information is usually obtained using a directional antenna or an antenna array [10], whereas the range information can be obtained from the received signal strength indication (RSSI) [11], round trip-of-flight (TOF) [12], time-difference-of-arrival (TDOA) [13], and/or phase-difference-of-arrival (PDOA) measurements [14]. Second, the location of the object is determined by utilizing such information in relation to multiple known reference points. These positioning methods include multilateration, multiangulation, and hybrid direction/range methods [15–18]. Other approaches for the localization of RFID-enabled objects include proximity and radio map matching. A survey of the state-of-the-art RFID localization techniques is presented in [2] and [19]. Selection of an appropriate localization algorithm is determined based on the resource constraints (e.g., bandwidth and power limitations), propagation conditions (e.g., indoor or outdoor), choice of RFID tags (e.g., active or passive), and other system limitations [20].

In RFID systems, localization of tags is a more customary problem (e.g., supply chain and transportation). In such applications, there are a large number of objects to be detected and localized. As such, each object is identified with a tag and multiple spatially distributed readers at known locations serving as reference points. On the other hand, when the number of objects of interest is limited as observed in, e.g., mobile robot localization [21] and path planning [22], the objects are identified using RFID readers, whereas the tags serve as the reference points. RFID reader localization is a dual problem commonly deployed for such applications. In this paper, we focus on the localization of an RFID reader by exploiting the RSSI measurements obtained from multiple spatially distributed passive tags as the only form of observation.

In complex propagation conditions due to, e.g., multipath propagation or non-isotropic radiation of the reader and tag antennas, the one-to-one correspondence cannot be guaranteed between the observed signal and the range information, rendering compromised localization accuracy [20]. Different approaches have been proposed to mitigate the effect of multipath propagation on range estimation and, consequently, on RFID localization. For example, frequency hopping method [23], averaging over multiple frequency pairs in phase-based methods, and ultra-wideband signaling [2] are deployed for improved localization. In time-invariant propagation environments, localization algorithms based on radio map matching or scene analysis, such as LANDMARC [24] and its variants, are known to be less sensitive to such propagation impairments as these factors are incorporated into the pre-stored radio map. Some recent works in through-the-wall radar have coined 'multipath exploitation' (e.g., through-the-wall target localization with a single sensor [25] and through-the-wall radar imaging based on group sparse reconstruction [26]), by using the prior information regarding the multipath geometry to their advantage. Likewise, the compensation for the non-isotropic radiation pattern is proposed in [27], before the measurements

This work is supported in part by the Office of Naval Research under grant N00014-16-1-2425.

S. Subedi and E. Pauls are with the Center for Advanced Communications, Villanova University, Villanova, PA 19085 USA.

Y. D. Zhang is with the Department of Electrical and Computer Engineering, Temple University, Philadelphia, PA 19122, USA. E-mail: ydzhang@temple.edu.

are exploited for range and/or DOA estimation. The need for compensating for the effects of multipath propagation and non-isotropic radiation field pattern is also established in [20, 28], and the *a priori* knowledge about the propagation environment is exploited to compensate for their effects.

Recently, odometry and vehicle information are employed as a supplemental source of information to further improve the accuracy of localization [29–32]. For instance, the motion-continuity property of differential-driving mobile robots is utilized in [29]. In [30, 31], the orientation of an RFID enabled vehicle is employed as an additional prior. Information from two heterogeneous sensors, namely, RFID sensors and wheel encoders, is fused in [32] to improve the accuracy of localization.

In this paper, we focus on the localization of a single RFID reader in a two-dimensional (2-D) space by exploiting the RSSI measurements obtained from multiple spatially distributed passive tags. The key contributions of this work are summarized in the following;

1) We provide a comprehensive analysis of the individual and combined effects of multipath propagation and non-isotropic radiation pattern of the reader antenna on the localization performance.
2) We apply the maximum likelihood (ML) estimation based method to obtain an optimum localization at a low computational cost. The ML estimation based method offers two distinct advantages compared to traditional approaches: (a) It does not require an intermediate step of range estimation, which is the main source of error in the traditional method; and (b) It accurately models the propagation environment and effectively compensates for the effects of the propagation impairments.
3) Subsequently, the position estimates obtained in the form of 2-D Cartesian coordinates of the reader position and its velocity are then used as inputs to a Kalman filter for dynamically estimating the trajectory of the reader within the surveillance region.
4) We deploy the proposed algorithm in a realistic propagation environment. Experimental results corroborate that, due to the ability to compensate for the channel impairments and incorporate supplemental vehicle information at a low computational cost, the proposed method significantly improves the accuracy, by an order of magnitude, compared to the state-of-the-art techniques for similar applications [29–33] under a comparable density of tag deployment.

Notations: A lower (upper) case bold letter denotes a vector (matrix). Specifically, $\mathbf{I}_N$ and $\mathbf{0}_N$ denote the $N \times N$ identity and zero matrices, respectively. $(.)^T$ and $(.)^H$, respectively, denote transpose and hermitian operations, and $\circ$ denotes the Hadamard product. $\mathbb{R}^{n\times 1}$ and $\mathbb{C}^{n\times 1}$, respectively, represent the n-dimensional real and complex vectors. $\|\cdot\|_n$ denotes the l_n-norm of a vector, and $x \sim \mathcal{N}(a,b)$ denotes variable x to be Gaussian distributed with mean a and variance b.

The remainder of this paper is organized as follows. Section II describes the RFID reader-tag grid configuration and formulate the RSSI expressions with the consideration of non-isotropic radiation pattern of tag antennas, multipath propagation, and measurement errors. Section III briefly introduces the conventional RSSI-based passive RFID reader localization technique through multilateration. Section IV models the problem as an ML estimation problem and proposes a method to accurately estimate the location of a reader in a 2-D space by compensating for the effects of the propagation impairments. Section V presents the use of Kalman filter for dynamically estimating the trajectory of the reader by exploiting the instantaneous position estimates as the input. Section VI provides the experimental results and a comparison of the estimation accuracy achieved by exploiting the proposed method against the state-of-the-art for similar applications. Finally, conclusions are drawn in Section VII.

II. Signal Model

We consider a passive RFID system comprising K passive RFID tags distributed in a predefined arrangement over a rectangular search area and a reader as shown in Fig. 1. For the underlying problem of reader localization, tags are assumed to be located at known positions and serve as the reference points. The position of the kth tag in a 3-D space is defined as $\mathbf{t}_k \triangleq [t_{xk}, t_{yk}, t_{zk}]^T$. At each tag position $\mathbf{t}_k$, we use an orthogonal pair of tags to form a 'super-tag' arrangement. The concept of super-tag is introduced in [34] where multiple tags are deployed at the same location but with different orientations. Such orientation diversity ensures that at least one tag is in an orientation of a high directive gain, thereby achieving a high likelihood of detecting tags for each tag location. Our earlier empirical study [28] also implemented super-tags in the form of a pair of orthogonal tags.

The reader is assumed to be moving along a trajectory within the rectangular search area with a velocity $\mathbf{v}_\tau$. The reader position at the τth observation instant is defined as $\mathbf{q}_\tau \triangleq [q_{x,\tau}, q_{y,\tau}, q_{z,\tau}]^T$. The tags are assumed to be located on the flat floor whereas the reader is placed at a known and fixed height of h above the ground. As such, the reader localization is reduced to a 2-D problem. We consider the problem of tracking the reader over T observation instants, i.e., $\tau = 1, \cdots, T$. At each observation instant, we discard the tags that do not respond or report RSSI values below a certain threshold. As such, for the τth observation, the actual number of tags contributing towards localization, L_τ, is much smaller than K.

Since passive RFID tags are not equipped with built-in energy sources, they rely on the radio frequency power transmitted from the reader to activate their internal circuitry and respond back to the reader. As such, the signal transmitted from a reader propagates twice along the propagation path. According to the Friis transmission equation, for the τth observation instant, the signal power received at the reader due to the signal backscattered from the kth tag is expressed as [35]

$$p_{k,\tau} = p_{\mathrm{Tx}} G^2_{\mathrm{t},k,\tau} G^2_{\mathrm{r},k,\tau} \zeta \left(\frac{\lambda}{4\pi d_{k,\tau}} \right)^{2\eta}, \qquad (1)$$

where p_{Tx} is the transmit power from the reader, $G_{\mathrm{t},k,\tau}$ and $G_{\mathrm{r},k,\tau}$ are the directional gains of the kth tag, and reader

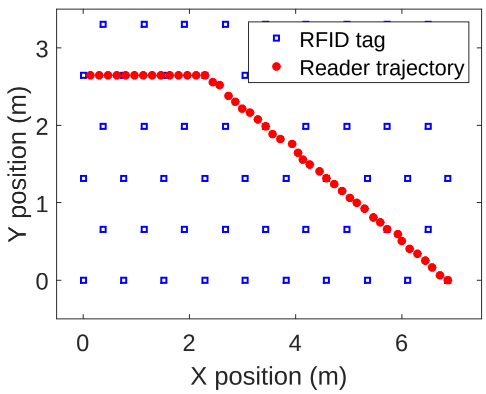

Fig. 1. Tag distribution and reader trajectory.

antenna, respectively, in the direction of propagation, ζ is the backscatter transmission efficiency of the passive tag, λ is the wavelength of the transmitted signal, and $d_{k,\tau}$ is the range between the kth tag and the reader during the τth time instant. The tag efficiency, ζ, is generally considered constant which typically takes a value of -5 dB [35] but can be adjusted empirically based on the measured data [28]. The path loss exponent, η, varies depending upon the propagation environment. Considering that the reader has line-of-sight (LOS) with the tags, free space propagation is assumed and, as such, η is assumed to be 2. However, other values empirically estimated for a given propagation environment can also be used. As such, for LOS propagation and known antenna gains of the reader and the tag antennas in the direction of propagation, the range between the reader and the kth tag at the τth observation can be estimated from the RSSI measurements as follows,

$$\breve{d}_{k,\tau} = \left(\frac{\lambda}{4\pi}\right)\left(\frac{p_{\mathrm{Tx}} G^2_{\mathrm{t},k,\tau} G^2_{\mathrm{r},k,\tau}}{p_{k,\tau}}\right)^{\frac{1}{4}}. \tag{2}$$

In practice, however, the actual directional gains of the reader and the tag antennas towards the respective propagation directions depend on their relative positions and, hence, are unknown *a priori*.

Since the RFID systems are typically operated over a short distance, the RSSI measurements are highly coupled with the reader and tag antenna patterns [27]. Therefore, the range estimates may become ambiguous in the presence of non-isotropic radiation patterns. Multipath propagation is another major source of error in RSSI based localization. The signals propagating along different paths are superposed at the RFID reader, constructively or destructively, depending on their relative phases. This causes significant variations in signal strength even within a fraction of a wavelength, which adds to the ambiguity in range estimates calculated on the basis of RSSI measurements.

In the following, we separately analyze the effects of multipath propagation and directional pattern of the reader antenna on range estimates, and consequently, on reader localization performance.

A. Effect of multipath propagation

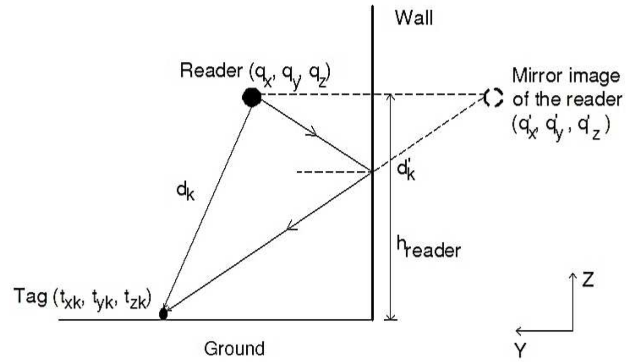

Fig. 2. Two-ray reflection model.

Multipath propagation, due to the presence of different reflecting and scattering objects in the propagation scene, can be a major source of error in RFID reader localization. In many practical applications, the geometry of the significant reflectors is either known or can be pre-estimated. For example, in a recent work [36], a low-complexity clustering algorithm is developed to detect multiple reflectors and estimate their geometry using time delay measurements. We consider a case where the reflector is a flat vertical surface with a known position. Such situations arise, for example, when the reader is mounted on a vehicle in a warehouse with a reflective surface, whereas other reflectors are distant from the vehicle. In such a situation, signal transmitted from a reader follows two distinct paths: a direct path and a reflection path, as illustrated in Fig. 2. The analysis presented here can be easily extended to a multiple reflector scenario. Signals can also propagate through multiple reflections but they are severely attenuated and, hence, become negligible in the RSSI measurement. Along the direct path, the propagation distance between the reader and the kth tag at the τth observation equals $d_{k,\tau} = ||\mathbf{q}_\tau - \mathbf{t}_k||$. Similarly, along the reflection path, the propagation distance equals $\tilde{d}_{k,\tau} = ||\tilde{\mathbf{q}}_\tau - \mathbf{t}_k||$, where $\tilde{\mathbf{q}}_\tau$ is the mirror image of the reader position about the reflecting surface (see Fig. 2). Therefore, the path difference between the direct path and the reflection path is

$$\Delta d_{k,\tau} = \tilde{d}_{k,\tau} - d_{k,\tau}, \tag{3}$$

and the corresponding phase difference is

$$\Delta\alpha_{k,\tau} = \frac{2\pi}{\lambda}\Delta d_{k,\tau}. \tag{4}$$

Thus, following the ground two-ray model [37], the signal power backscattered to the reader from the kth tag can be expressed as

$$p_{k,\tau} = p_{\mathrm{Tx}}\left(\frac{\lambda}{4\pi}\right)^4\left|\frac{1}{d_{k,\tau}} + \frac{\Gamma\exp(-j\Delta\alpha_{k,\tau})}{\tilde{d}_{k,\tau}}\right|^4, \tag{5}$$

where Γ is the reflection coefficient of the wall. The phase interaction between two multipath components creates ambiguity in relation between the RSSI value observed at the reader and distance between the corresponding reader-tag pair. Therefore, in order to unambiguously estimate the propagation range by using the RSSI information available at the reader from multiple reference tag positions, it is important to compensate for the effects of all significant multipath components.

B. Effect of tag antenna directivity

Conventionally, RSSI-based localization algorithms assume isotropic radiation patterns for the reader and the tag antennas [38]. However, in practice, the effective radiation pattern is non-isotropic creating a bias towards the direction of high gain in the radiation pattern. In this paper, we only consider the effect of tag antenna pattern because the antenna gain does not change significantly within the main lobe of the radiation pattern of the reader antenna. Also, the tags located away from the main lobe of the the reader antenna do not report RSSI measurements above the preset threshold and are not accounted for localization. For notational purpose, this point onwards, we use $G_{k,\tau}$ to represent the directional gain of the kth tag antenna towards the direction of the reader antenna at the τth observation instant.

The effect of the tag antenna pattern is negligible in the far-field. However, because RFID systems are often operated in the near field, the tag antenna gain depends on the relative position between the reader and the tag and, as such, the spatial directivity has a pronounced effect on the RSSI measurements [27]. Therefore, it is required to compensate for the effect of directional radiation pattern on RSSI measurements when estimating the range. Incorporating the effects of tag antenna directivity in (5), the power backscattered to the reader from the kth tag can be modeled as

$$p_{k,\tau} = p_{\mathrm{Tx}} \left(\frac{\lambda}{4\pi}\right)^4 \left| \frac{\sqrt{G_{k,\tau}}}{d_{k,\tau}} + \frac{\Gamma\sqrt{\tilde{G}_{k,\tau}}\exp(-j\Delta\alpha_{k,\tau})}{\tilde{d}_{k,\tau}} \right|^4, \tag{6}$$

where $\tilde{G}_{k,\tau}$ represents the tag antenna gain along the reflection path.

C. Effect of RSSI measurement error

From a practical standpoint, statistic and systematic errors that occur during the RSSI measurement introduce another significant source of error in RSSI-based range estimation. In most of the RFID localization applications, a fairly high signal strength is maintained, and thus, these RSSI measurement errors are more significant than the thermal noise. Considering the effects of multipath propagation, tag antenna directivity, and the RSSI measurement error, the received signal at the RFID reader is expressed as

$$g_{k,\tau} = p_{k,\tau} + e_{k,\tau}, \tag{7}$$

where $p_{k,\tau}$ is the noise free power of the backscatter signal from the kth tag, and $e_{k,\tau}$ represents a RSSI measurement error modeled as an additive white Gaussian random variable $e_{k,\tau} \sim \mathcal{N}(0, \sigma^2_{ek,\tau})$.

In the following section, we review the conventional method of RSSI-based RFID reader localization through multilateration and evaluate its performance in the presence of propagation impairments.

III. RSSI-BASED LOCALIZATION VIA MULTILATERATION

Following (2), at the τth observation, the range between the reader and the kth tag can be estimated from the RSSI measurements as follows,

$$\hat{d}_{k,\tau} = \left(\frac{\lambda}{4\pi}\right)\left(\frac{p_{\mathrm{Tx}}}{g_{k,\tau}}\right)^{\frac{1}{4}}, \tag{8}$$

where the RSSI measurement from the kth tag $g_{k,\tau}$ is defined in (7). In order to unambiguously localize a reader in an n-dimensional space using multilateration, range information from at least $n+1$ tags is required. For the underlying problem, at the τth observation, we consider estimating the position of a single RFID reader in a 2-D space, such that

$$(q_{x,\tau} - t_{xk})^2 + (q_{y,\tau} - t_{yk})^2 + h^2 = \hat{d}^2_{k,\tau}, \quad k = 1, 2, ..., L_\tau, \tag{9}$$

where $L_\tau \geq 3$ and $\hat{d}_{k,\tau}$ is the propagation range estimated using (8). Availability of more number of tags results in an over-determined problem, which helps improving the accuracy of estimation.

After simple algebraic manipulations, equation (9) can be used to formulate the following linear relationship [2],

$$\mathbf{A}_\tau \mathbf{q}_\tau = \mathbf{b}_\tau, \tag{10}$$

where $\mathbf{q}_\tau = [q_{x,\tau}, q_{y,\tau}]^T$,

$$\mathbf{A}_\tau = \begin{pmatrix} t_{x1} - t_{x2} & t_{y1} - t_{y2} \\ \vdots & \vdots \\ t_{x(L_\tau-1)} - t_{xL_\tau} & t_{y(L_\tau-1)} - t_{yL_\tau} \end{pmatrix} \tag{11}$$

is a $(L_\tau-1)\times 2$ matrix, $\mathbf{b}_\tau \triangleq [b_1, \cdots, b_{L_\tau-1}]^T$ is a $(L_\tau-1)\times 1$ vector, and

$$b_{k,\tau} = \frac{1}{2}\Big((\hat{d}^2_{k+1,\tau} - \hat{d}^2_{k,\tau}) - (t^2_{x(k+1)} - t^2_{xk}) - (t^2_{y(k+1)} - t^2_{yk})\Big), \tag{12}$$

$k = 1, ..., L_\tau - 1$. Assuming that $L_\tau \geq 3$ and the tags are not collinearly located, the least square (LS) estimate of the x- and y-coordinates of the RFID reader position can be obtained as [2]

$$\hat{\mathbf{q}}^{(LS)}_\tau = (\mathbf{A}^T_\tau \mathbf{A}_\tau)^{-1}\mathbf{A}^T_\tau \mathbf{b}_\tau, \tag{13}$$

by minimizing the LS cost function

$$J(\mathbf{q}_\tau) = (\mathbf{b}_\tau - \mathbf{A}_\tau \mathbf{q}_\tau)^T(\mathbf{b}_\tau - \mathbf{A}_\tau \mathbf{q}_\tau). \tag{14}$$

As such, the estimated reader position is

$$\hat{\mathbf{q}}^{(LS)}_\tau = [\hat{\mathbf{q}}^{(LS)T}_\tau, h]^T. \tag{15}$$

As discussed in Section I, due to multipath propagation, tag antenna directivity, and RSSI measurement error, the relation between the reader-tag distance and the corresponding RSSI measurement is not consistent. As such, the accuracy of the LS estimate of the reader position is adversely affected due to these propagation impairments. Furthermore, it is not possible to compensate for the effects of such impairments using the multilateration based method. In the following section, we propose an ML estimation method, which does not involve an intermediate range estimation process and allows for an effective compensation of the effect of the propagation impairments to obtain an optimal solution.

IV. Precise Localization using ML estimation

From (7), we can infer that the $L_\tau \times 1$ received signal vector $\mathbf{g}_\tau \triangleq [g_1, \cdots, g_{L_\tau}]^T$ follows a multivariate normal distribution, i.e.,

$$\mathbf{g}_\tau \sim \mathcal{N}(\mathbf{p}_\tau, \mathbf{C}_\tau), \tag{16}$$

where $\mathbf{p}_\tau \triangleq [p_1, \cdots, p_{L_\tau}]^T$ is the $L_\tau \times 1$ mean vector, and $\mathbf{C}_\tau$ is the corresponding $L_\tau \times L_\tau$ covariance matrix. The 2×1 unknown vector $\mathbf{q}_\tau = [q_{x,\tau}, q_{y,\tau}]^T$ structures the mean value vector $\mathbf{p}_\tau(\mathbf{q}_\tau)$ according to a known function defined in (6). The covariance matrix, on the other hand, represents the effect of the RSSI measurement error modeled as an additive white Gaussian variable.

The log-likelihood function of the unknown vector $\mathbf{q}_\tau$ structuring the received signal vector $\mathbf{g}_\tau$ modeled as (16) is given as

$$\mathcal{L}(\mathbf{q}_\tau|\mathbf{g}_\tau) = -\frac{1}{2}\ln(\det(\mathbf{C}_\tau)) - \frac{1}{2}(\mathbf{g}_\tau - \mathbf{p}_\tau(\mathbf{q}_\tau))^T \mathbf{C}_\tau^{-1}(\mathbf{g}_\tau - \mathbf{p}_\tau(\mathbf{q}_\tau)), \tag{17}$$

and the corresponding ML estimate $\hat{\mathbf{q}_\tau}^{(ML)}$ is given as

$$\hat{\mathbf{q}}_\tau^{(ML)} = \arg \max_{\mathbf{q}_\tau \in \Xi} \mathcal{L}(\mathbf{q}_\tau|\mathbf{g}_\tau), \tag{18}$$

where Ξ represents all the points within the search area.

For a hypothetical reader position $\mathbf{q}_i = [q_{xi}, q_{yi}]^T$ within the 2-D search area, the error-free power measurement from the kth tag located at $\mathbf{t}_k$ is modeled, following (6), as

$$p_{k,i} = p_{\mathrm{Tx}} \left(\frac{\lambda}{4\pi}\right)^4 \left| \frac{\sqrt{G_{k,i}}}{d_{k,i}} + \frac{\Gamma\sqrt{\tilde{G}_{k,i}}\exp(-j\Delta\alpha_{k,i})}{\tilde{d}_{k,i}} \right|^4, \tag{19}$$

where $\tilde{G}_k$ represents the reader antenna gain along the reflection path. where $G_{k,i}$ and $\tilde{G}_{k,i}$, respectively, represent the directional gains of the reader antenna, hypothetically located at $\mathbf{q}_i = [\mathbf{q}_i^T, h]^T$, towards the tag located at $\mathbf{t}_k$ along the direct path and the reflection path. Likewise, $d_{k,i} = ||\mathbf{q}_i - \mathbf{t}_k||$ and $\tilde{d}_{k,i} = ||\tilde{\mathbf{q}}_i - \mathbf{t}_k||$, respectively, represent the distance between the hypothetical reader position and the kth tag along the direct path and the reflection path, and $\Delta\alpha_{k,i} = \frac{2\pi}{\lambda}\left(\tilde{d}_{k,i} - d_{k,i}\right)$, is the corresponding phase difference. Equation (19) represents an accurate model of the propagation environment, by exploiting the *a priori* knowledge of the radiation pattern of the reader antenna and multipath due to the presence of the wall in the propagation scene. As such, we can reformulate the underlying estimation problem in (18) as

$$\hat{\mathbf{q}}_\tau^{(ML)} = \arg \min_{\mathbf{q}_i} ||\mathbf{g}_\tau - \boldsymbol{\psi}_i(\mathbf{q}_i)||^2, \tag{20}$$

where the $L_\tau \times 1$ vector $\boldsymbol{\psi}_i \triangleq [p_{1,i}, \cdots, p_{k,i}, \cdots, p_{L_\tau,i}]^T$.

In the following section, we feed the ML estimate of the instantaneous reader position obtained from (20) to the Kalman filter for estimating the trajectory of the reader.

V. Kalman filtering

For tracking the trajectory of the reader, we resort to the Kalman filter. We define the state vector of the reader at the τth observation as a four-dimensional (4-D) vector $\mathbf{x}_\tau = [\mathbf{q}_\tau^T, \mathbf{v}_\tau^T]^T$ comprising its position $\mathbf{q}_\tau \triangleq [q_{x,\tau}, q_{y,\tau}]^T$ and velocity $\mathbf{v}_\tau \triangleq [v_{x,\tau}, v_{y,\tau}]^T$ in the two-dimensional (2-D) Cartesian coordinate system. The reader dynamics is assumed to evolve according to a constant velocity linear Gaussian model, such that

$$\mathbf{x}_\tau = \mathbf{F}\mathbf{x}_{\tau-1} + \mathbf{w}_{\tau-1}, \tag{21}$$

where $\mathbf{F}$ is the state transition matrix defining the linear dynamics, expressed as

$$\mathbf{F} = \begin{bmatrix} \mathbf{I}_2 & \Delta\mathbf{I}_2 \\ \mathbf{0}_2 & \mathbf{I}_2 \end{bmatrix}, \tag{22}$$

Δ is the sampling interval, and $\mathbf{w}_\tau \sim \mathcal{N}(\mathbf{0}, \mathbf{Q})$ is the process noise modeled as additive white Gaussian. The process noise covariance matrix can be expressed as

$$\mathbf{Q} = \sigma_{\mathbf{w}}^2 \begin{bmatrix} \frac{\Delta^3}{3}\mathbf{I}_2 & \frac{\Delta^2}{2}\mathbf{I}_2 \\ \frac{\Delta^2}{2}\mathbf{I}_2 & \Delta\mathbf{I}_2 \end{bmatrix}, \tag{23}$$

where $\sigma_{\mathbf{w}}^2$ is the variance of the process noise.

For each observation instant, τ, we feed the ML estimates of the instantaneous reader position as a measurement to the Kalman filter. We define the measurement vector as $\mathbf{z}_\tau = [\hat{\mathbf{q}}_\tau^{(ML)T}, \mathbf{v}_\tau^T]^T$, where $\hat{\mathbf{q}}_\tau^{(ML)}$ is the ML estimate of the instantaneous reader position obtained from (20). Since this is a self-localization problem, we assume the prior knowledge of the instantaneous velocity. As such, we can define the measurement vector as

$$\mathbf{z}_\tau = \mathbf{H}_\tau\mathbf{x}_\tau + \eta_\tau, \tag{24}$$

where $\mathbf{H}_\tau = \mathbf{I}_4$ is the matrix mapping the measurement to the target state space and $\eta_\tau \sim \mathcal{N}(\mathbf{0}, \mathbf{R}_\tau)$ is the measurement noise modeled as an additive white Gaussian vector. As such, following the conventional Kalman filter formulations [39], we obtain the predictions for the state vector and the corresponding covariance matrix, respectively, as

$$\hat{\mathbf{x}}_{\tau|\tau-1} = \mathbf{F}\hat{\mathbf{x}}_{\tau-1|\tau-1}, \tag{25}$$

and

$$\mathbf{P}_{\tau|\tau-1} = \mathbf{Q}_{\tau-1} + \mathbf{F}\mathbf{P}_{\tau-1|\tau-1}\mathbf{F}^T. \tag{26}$$

Likewise, the updates are obtained as

$$\hat{\mathbf{x}}_{\tau|\tau} = \hat{\mathbf{x}}_{\tau|\tau-1} + \mathbf{K}_\tau\left(\mathbf{z}_\tau - \mathbf{H}_\tau\hat{\mathbf{x}}_{\tau|\tau-1}\right), \tag{27}$$

and

$$\mathbf{P}_{\tau|\tau} = \mathbf{P}_{\tau|\tau-1} - \mathbf{K}_\tau\mathbf{S}_\tau\mathbf{K}_\tau^T, \tag{28}$$

where $\mathbf{S}_\tau$ is the covariance of the innovation term $\mathbf{s}_\tau = \mathbf{z}_\tau - \mathbf{H}_\tau\hat{\mathbf{x}}_{\tau|\tau-1}$, and $\mathbf{K}_\tau = \mathbf{P}_{\tau|\tau-1}\mathbf{H}_\tau^T\mathbf{S}_\tau^{-1}$ represents the Kalman gain.

VI. Experimental results

In this section, we present the experimental study results to validate the proposed algorithm. For the experiments, we use an Alien ALR-9680 RFID reader with transmit power of 1W (30 dBm) communicating in the ultra high frequency (UHF) frequency band between $902.75 - 927.25$ MHz. The reader is connected to a Poynting PatchA0026 right-hand circularly polarized antenna with a nominal gain of 6.5 dBi (± 0.5 dB) and 3 dB beamwidth of $60°$ ($\pm 5°$) and $74°$ ($\pm 5°$) in elevation

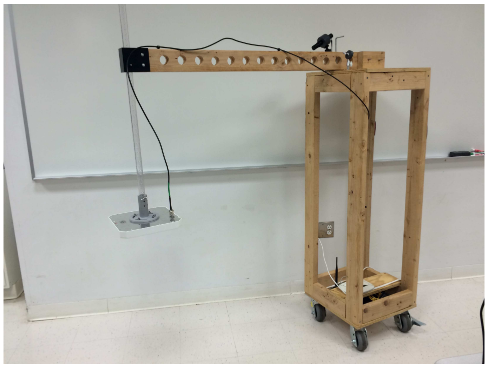

Fig. 3. Structure hosting the RFID reader.

Fig. 4. Experiment setup.

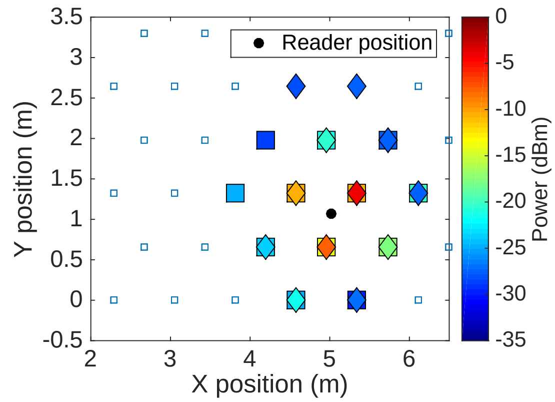

Fig. 5. RSSI map illustrating the effect of tag antenna orientation.

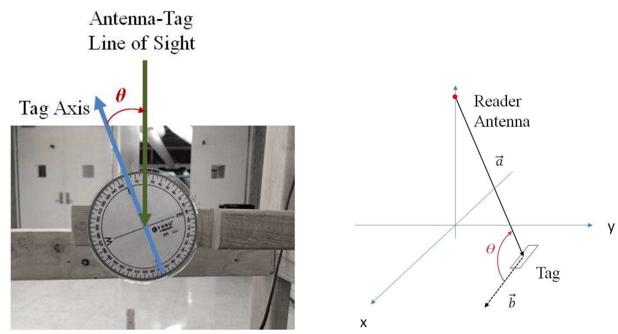

(a) (b)

Fig. 6. Experiment for estimating the radiation pattern of the tag antenna (a) Experimental setup. (b) Illustration of tag orientation angle.

and azimuth, respectively. Alien Squiggle Higgs3 passive UHF RFID tags are used for the experiments.

The RFID reader antenna is mounted at a fixed height of approximately 0.88 m onto a movable wooden structure, as shown in Fig. 3, and the tags are distributed at 57 fixed locations on a carpet over a concrete surface at a minimum tag spacing of 0.762 m in an arrangement comprising contiguous equilateral triangles, as depicted in Fig. 4. In order to account for the non-linear artifacts, including tag efficiency, we prescreen tags such that only those that generate consistently similar RSSI measurements in a controlled test environment [28] are used for the experiment. The wooden structure hosting the RFID reader antenna moves along a trajectory comprising 46 points within a designated surveillance area where the tags are arranged in a fixed pattern. As discussed in Section II, for each observation instant τ, we discard the tags that report RSSI values below -104 dBm. It was observed empirically that the RSSI values below this threshold suffer from a high variance, rendering the measurements unreliable for localization. Similar observations were reported in [28]. As such, the actual number of tags contributing towards localization is different for each observation instant τ. The experiment is conducted in a large patio devoid of any significant reflecting objects in the close vicinity of the experimental setup.

A. *Effect of tag antenna directivity*

An example of the RSSI map observed at the reader is presented in Fig. 5. This figure clearly demonstrates the effect of the radiation pattern of the tag antenna on the RSSI measurements. The squares and diamonds respectively show RSSI results corresponding to the two orthogonally oriented tags. It is evident that the two tags arranged as an orthogonal pair report significantly different RSSI values depending on their respective orientation even though they are located exactly at the same distance from the reader. Also, the RSSI values reported from equidistant tags located towards different directions from the reader are different. This empirical observation corroborates the analysis in Section II and illustrates the need for compensating for the effect of non-isotropic radiation pattern of the tag antenna.

In order to accurately compensate for the effect of the non-isotropic radiation pattern of the tag antenna, we empirically estimate its radiation pattern. For the experiment, we place an RFID tag directly beneath the RFID reader antenna at a fixed distance of 0.76 m and rotate the tag in the range $[-90°, 90°]$ at an increment of $10°$ as shown in Fig. 6. The angle of rotation θ is the angle between the reader-tag line of sight vector $\mathbf{a}$ and the tag axis vector $\mathbf{b}$, as shown in Fig. 6(b), and is obtained as

$$\theta = \arccos\left(\frac{\mathbf{a}\cdot\mathbf{b}}{\|\mathbf{a}\|_2\|\mathbf{b}\|_2}\right). \tag{29}$$

The empirically estimated radiation pattern of the tag antenna is shown in Fig. 7, where it is evident that the directional gain is approximately constant over the range of $[-40°, 40°]$

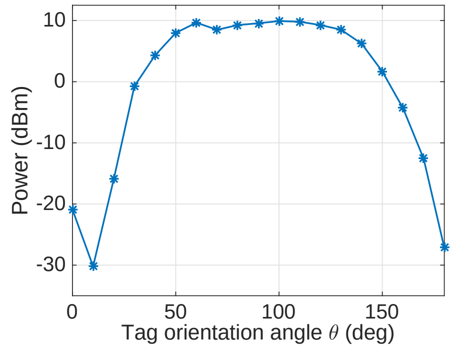

Fig. 7. Radiation pattern of the tag antenna.

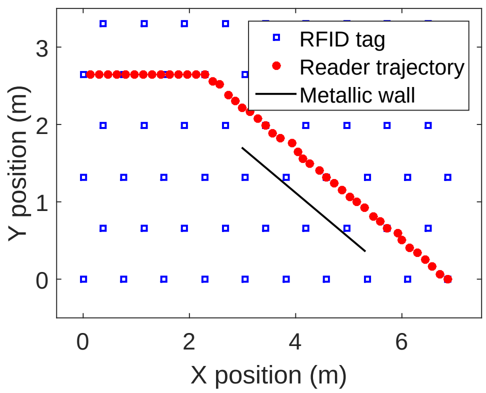

Fig. 8. Location of the metallic wall.

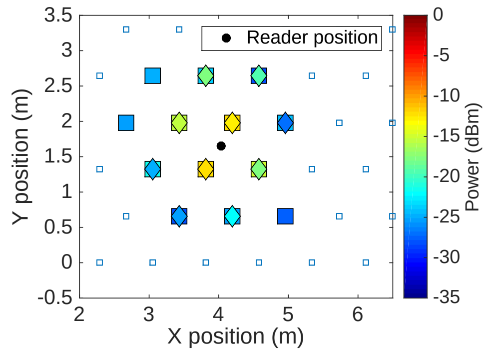

(a)

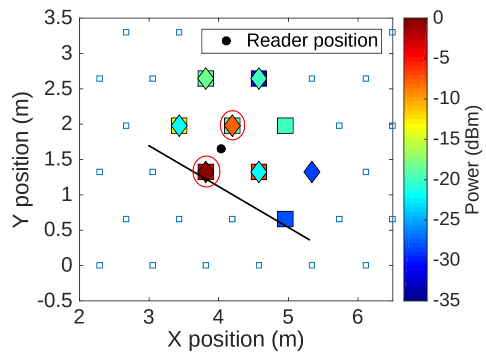

(b)

Fig. 9. RSSI map for a fixed reader position. (a) Without metallic wall. (b) With metallic wall.

and rapidly decreases outside this range. Empirical results verify that the radiation pattern of the Alien Squiggle Higgs3 passive UHF RFID tags [40] is toroidal and a higher gain is experienced along the bore-sight direction. Also, we can observe that the radiation pattern of the tag antenna is largely symmetric about the axis of rotation.

B. Effect of metallic wall

In order to investigate the effect of a reflecting surface inside the region of interest, a reflecting surface in the form of an aluminum plate of height 0.91 m between the points $(3, 1.694)$ m and $(5.3, 0.366)$ m as illustrated in Fig. 8. The wall is located parallel to the reader trajectory and is approximately at a vertical distance of 0.55 m from the reader trajectory. We compare the RSSI map observed at the reader at a fixed position with and without the metallic wall in Fig. 9. The presence of the reflecting surface within the read range of the reader creates a bias in the RSSI map. For example, the two tags (circled in red in Fig. 9(b)) located at an equal distance from the reader, report significantly different RSSI values due to the strong reflection from the metallic surface.

C. Comparison of multilateration and the ML based methods

First, we compare the estimated reader trajectories using the multilateration based method and the ML estimation based method without any compensation. The results in Figs. 10 and 11 show that the multilateration based location estimation process suffers significantly more than the ML estimation based method in the presence of the propagation impairments, i.e., non-isotropic radiation pattern and multipath propagation. This is primarily due to the intermediate range estimation process and a subsequent non-linear relationship between the estimated ranges and the reader position estimate.

While the ML estimation based method has a lower error compared to the multilateration based approach even without compensation as illustrated in Fig. 11. However, there is clearly a bias in location estimates towards the metallic wall because the RSSI measurement is sensitive to reflection. Fig. 12 shows that this error can be significantly reduced by properly modeling and compensating for the effects multipath propagation.

Next, we compare the reliability of location estimation for each point in the reader trajectory using the conventional multilateration based method and the proposed ML estimation based method in Fig. 13. Experimental results show that the proposed method achieves a significantly lower variance. As such, it not only improves the accuracy but also notably increases the consistency of location estimation by compensating for the effects of non-isotropic radiation pattern and multipath propagation.

D. Reader position tracking using Kalman filter

As discussed in Section V, we can further improve the estimation accuracy of the position of the RFID reader by exploiting the dynamic model assumed to be known *a priori*.

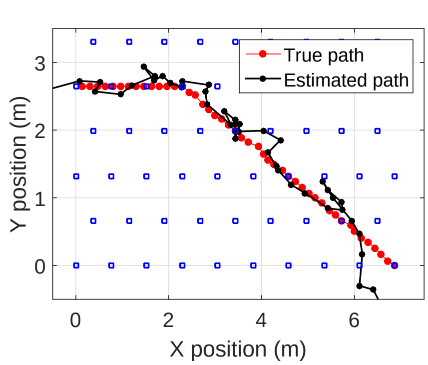

(a)

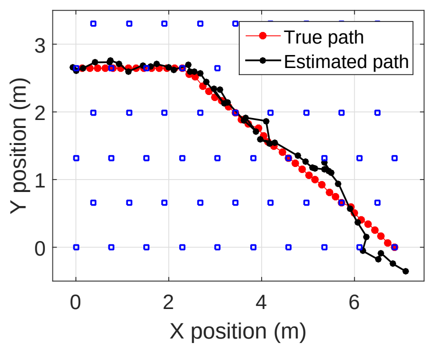

(b)

Fig. 10. Estimated reader trajectories without a metallic wall. (a) Multilateration based method. (b) ML estimation based method without compensation.

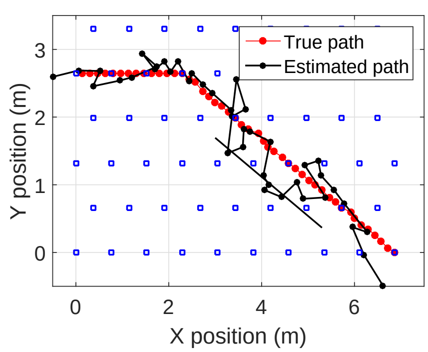

(a)

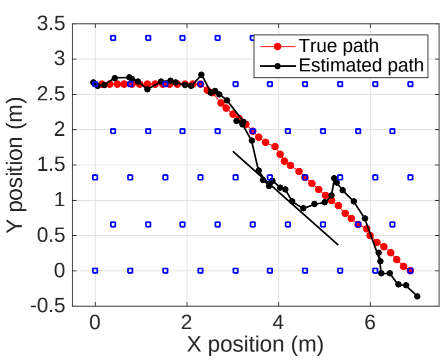

(b)

Fig. 11. Estimated reader trajectories with the metallic wall. (a) Multilateration based method. (b) ML estimation based method without compensation.

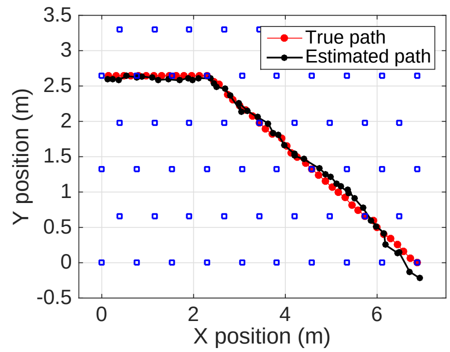

(a)

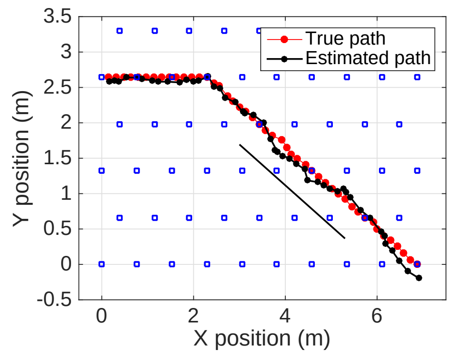

(b)

Fig. 12. Estimated reader trajectories using the ML method after compensation. (a) Without metallic wall. (b) With metallic wall.

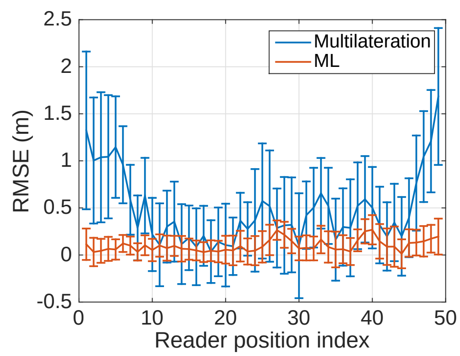

Fig. 13. Consistency of location estimation.

The estimated trajectory after Kalman filtering is shown in Fig. 14. It can be observed that the Kalman filter prevents sudden changes in the estimated trajectory by suppressing the ML position estimates that do not conform to the dynamic model. As such, the overall accuracy can be significantly improved at a low computational cost by exploiting the Kalman filter.

Specifically, in this experiment, the average root mean square error (RMSE) of the location estimates averaged over the 46 points along the reader trajectory is summarized in Table I. The RMSE of the location estimates of the conventional multilateration based method is approximately 0.45 m without wall, which degrades further to approximately 0.50 m in the presence of a metallic wall. The ML estimation based method reduces the error to as low as 0.1 m due to its ability

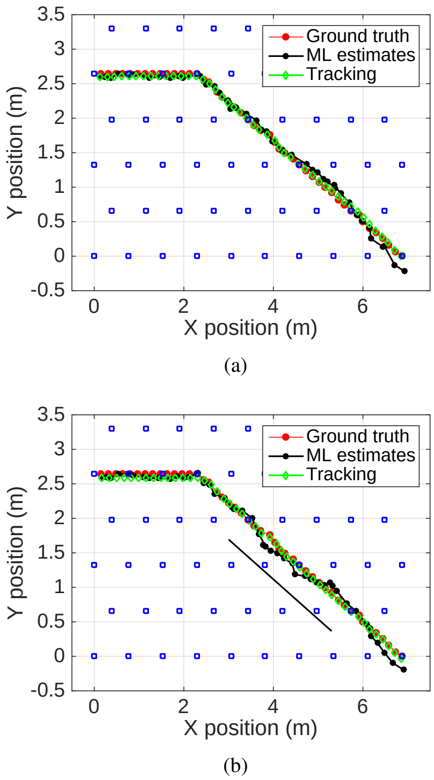

Fig. 14. Estimated reader trajectory after applying Kalman filter on ML estimates. (a) Without metallic wall. (b) With metallic wall.

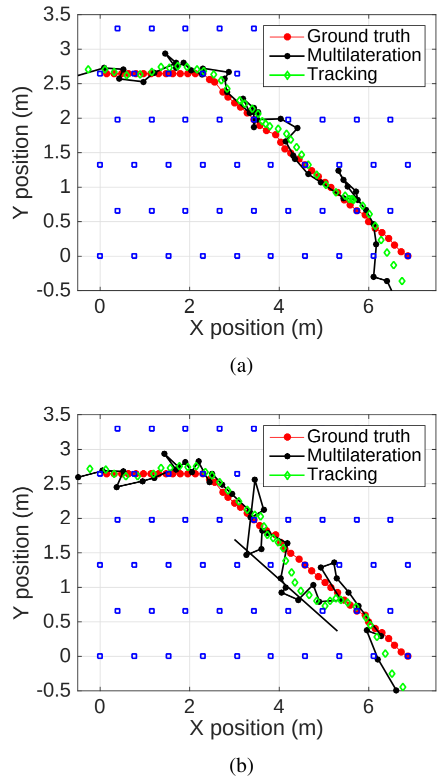

Fig. 15. Estimated reader trajectory after applying Kalman filter on LS estimates. (a) Without metallic wall. (b) With metallic wall.

to compensate for propagation impairments. Application of Kalman filtering on the output of ML estimates achieves an improved accuracy of less than 0.04 m by exploiting the prior knowledge of the reader's instantaneous velocity.

It is worthwhile to mention that, while the Kalman filter is a generic framework that can be applied in tandem with the conventional multilateration based approach as well, it is important to note that the primary source of error in the multilateration based method is its inability to correct for the artifacts of multipath propagation and antenna directivity. These propagation impairments manifest themselves as estimation bias and larger estimation variance, which are more difficult to mitigate by exploiting the Kalman filter as shown in Fig. 15.

E. Comparison with state-of-the-art methods

In Table II, we compare the accuracy of the proposed method with other state-of-the-art passive RFID localization methods [29–33]. It is noted that, as different methods used different tag grids with varying levels of tag densities, the localization accuracy has to be evaluated in relation to the the respective density of tag deployment and minimum tag spacing for fair comparison. We use the normalized error, defined as the product of the localization error and the respective tag density, i.e.,

$$e_{n,\tau} = \frac{\|\hat{\mathbf{q}}_\tau - \mathbf{q}_\tau\|_2^2}{A/K}, \tag{30}$$

as a basis of comparison in Table II, where $e_{n,\tau}$ is the normalized error, $\hat{\mathbf{q}}_\tau$ and $\mathbf{q}_\tau$ represent the estimated and true positions of the reader at the τth observation instant, A is the area of surveillance, and K represents the number of tags deployed. A comparison of the localization performance of these methods in terms of the normalized localization error shows that the proposed method outperforms other methods for a given tag density.

VII. Conclusion

In this paper, we have proposed an ML estimation technique to directly estimate the position of an RFID reader in a 2-D cartesian coordinates without the intermediate range estimation process. The proposed method allows us to compensate for the artifacts of the multipath propagation and the non-isotropic antenna pattern and obtain an optimal solution in the ML sense. We further apply the Kalman filter for dynamically estimating the trajectory of the reader within the surveillance region. Experimental results verified that the proposed algorithm outperforms the conventional multilateration based localization technique and the estimation accuracy is further improved at a low computational cost by exploiting the Kalman filter. A comparison of the localization performance of these methods in terms of the normalized localization error shows that the proposed method achieves significantly higher localization accuracy compared to other methods for a given tag density. Conversely, for a given accuracy, the proposed method requires a sparser tag deployment.

TABLE I
AVERAGE RMSE OF LOCALIZATION (IN m).

Propagation	Multilateration	ML estimation	Multilateration + KF	ML + KF
Without wall	0.443	0.095	0.263	0.031
With wall	0.484	0.098	0.292	0.039

TABLE II
COMPARISON OF LOCALIZATION ACCURACY OF THE STATE-OF-THE-ART USING RFID SYSTEMS.

Reference	Localization error (m)	Tags/m^2	Minimum tag spacing (m)	Normalized error (m)	Use odometry or vehicle information
[33]	0.049	400	0.05	19.60	No
[29]	0.009	400	0.05	3.60	Yes
[30]	0.145	8.65	0.34	1.25	Yes
[31]	0.014	11.56	0.294	0.16	Yes
[32]	0.010	11.11	0.3	0.11	Yes
Proposed	0.031	1.99	0.762	0.06	Yes

REFERENCES

[1] K. Finkenzeller, *RFID Handbook: Radio-Frequency Identification Fundamentals and Applications*, New York, NY: Wiley, 1999.

[2] Y. Zhang, X. Li, and M. G. Amin, “Principles and techniques of RFID positioning,” in *RFID Systems Research Trends and Challenges*, M. Bolić, D. Simplot-Ryl, I. Stojmenović, eds., New York, NY: Wiley, pp. 389–412, 2010.

[3] N. C. Karmakar, *Handbook of Smart Antennas for RFID Systems*, Hoboken, NJ: Wiley, 2011.

[4] C. Hekimian-Williams, B. Grant, L. Xiuwen, Z. Zhang, and P. Kumar, “Accurate localization of RFID tags using phase difference,” in *Proc. IEEE Int. Conf. RFID*, Orlando, FL, Apr. 2010, pp. 89–96.

[5] J. S. Choi, H. Lee, R. Elmasri, and D. W. Engels, “Localization systems using passive UHF RFID,” in *Proc. Int. Joint Conf. INC, IMS and IDC*, Seoul, Korea, Aug. 2009, pp. 1727–1732.

[6] D. Fortin-Simard, K. Bouchard, S. Gaboury, B. Bouchard, and A. Bouzouane, “Accurate passive RFID localization system for smart homes,” in *Proc. IEEE Int. Conf. Netw. Embed. Syst. for Every Appl.*, Liverpool, U.K., Dec. 2012, pp. 1–8.

[7] J. Maneesilp, W. Chong, W. Hongyi, and T. Nian-Feng, “RFID support for accurate 3D localization,” *IEEE Trans. Computers*, vol. 62, no. 7, pp. 1447–1459, July 2013.

[8] S. Chia, A. Zalzala, L. Zalzala, and A. Karim, “Intelligent technologies for self-sustaining, RFID-based, rural e-health systems,” *IEEE Technol. Soc. Mag.*, vol. 32, no. 1, pp. 36–43, 2013.

[9] T. Kanda, M. Shiomi, Z. Miyashita, H. Ishiguro, and N. Hagita, “A communication robot in a shopping mall,” *IEEE Trans. Robotics*, vol. 26, no. 5, pp. 897–913, Oct. 2010.

[10] Y. Zhang, M. G. Amin, and S. Kaushik, “Localization and tracking of passive RFID tags based on direction estimation,” *Int. J. Antennas Propagat.*, vol. 2007, article ID 17426, Dec. 2007.

[11] G. Marrocco, E. Di Giampaolo, and R. Aliberti, “Estimation of UHF RFID reading regions in real environments,” *IEEE Antennas Propagat. Mag.*, vol. 51, no. 6, pp. 44–57, Dec. 2009.

[12] F. Izquierdo, M. Ciurana, F. Barcelo, J. Paradells, and E. Zola, “Performance evaluation of a TOA-based trilateration method to locate terminals in WLAN,” in *Proc. Int. Symp. Wireless Pervasive Comput.*, Phuket, Thailand, Jan. 2006, pp. 1–6.

[13] T. Wang, “Novel sensor location scheme using time-of-arrival estimates,” *IET Signal Process.*, vol. 6, no. 1, pp. 8–13, Feb. 2012.

[14] X. Li, Y. Zhang, and M. G. Amin, “Multifrequency-based range estimation of RFID tags,” in *Proc. IEEE Int. Conf. RFID*, Orlando, FL, Apr. 2009, pp. 147–154.

[15] A. H. Sayed, A. Tarughat, and N. Khajehnouri, “Network-based wireless location: challenges faced in developing techniques for accurate wireless location information,” *IEEE Signal Process. Mag.*, vol. 22, no. 4, pp. 24–40, July 2005.

[16] A. Milella, P. Vanadia, G. Cicirelli, and A. Distante, “RFID-based environment mapping for autonomous mobile robot applications,” in *Proc. IEEE/ASME Int. Conf. Adv. Intell. Mechatron.*, Zurich, Switzerland, Sept. 2007, pp. 1–6.

[17] J. Song, C. T. Haas, and C. H. Caldas, “A proximity-based method for locating RFID tagged objects,” *Advanced Engineering Informatics*, vol. 21, no. 4, pp. 367-376, Oct. 2007.

[18] Y. D. Zhang, X. Li, and M. G. Amin, “Array processing for RFID tag localization exploiting multi-frequency signals,” in *Proc. SPIE*, vol. 7349, Orlando, FL, Apr. 2009.

[19] M. Bouet and A. L. Dos Santos, “RFID tags: Positioning principles and localization techniques,” in *Proc. IFIP Wireless Days Conf.*, Dubai, UAE, Nov. 2008, pp. 1–5.

[20] S. Subedi, Y. D. Zhang, and M. G. Amin, “Precise RFID localization in impaired environment through sparse signal recovery,” in *Proc. SPIE*, vol. 8753, Baltimore, MD, May 2013.

[21] K. Yamano, K. Tanaka, M. Hirayama, E. Kondo, Y. Kimuro, and M. Matsumoto, “Self-localization of mobile robots with RFID system by using support vector machine,” in *Proc. IEEE/RSJ Int. Conf. Intell. Robots and Syst.*, vol. 4, Sendai, Japan, Sept. 2004, pp. 3756–3761.

[22] S. A. Parkison, E. T. Psota, and L. C. Perez, “Automated indoor RFID inventorying using a self-guided micro-aerial vehicle,” in *Proc. IEEE Int. Conf. Electro/Inf. Technol.*, Milwaukee, WI, Jun. 2014, pp. 335–340.

[23] I. Amir and A. Naim, “Frequency hopping range estimation with low power consumption,” US Patent, 7061428 B1.

[24] L. M. Ni, Y. Liu, Y. C. Lau, and A. P. Patil, “LANDMARC: indoor location sensing using active RFID,” in *Proc. IEEE Int. Conf. Pervasive Comput. and Commun.*, Dallas-FortWorth, TX, Mar. 2003, pp. 407–415.

[25] P. Setlur, G. E. Smith, F. Ahmad and M. G. Amin, “Target localization with a single sensor via multipath exploitation,” *IEEE Trans. Aerosp. and Electron. Syst.*, vol. 48, no. 3, pp. 1996–2014, Jul. 2012.

[26] Q. Wu, Y. D. Zhang, M. G. Amin, and F. Ahmad, “Through-the-wall radar imaging based on modified Bayesian compressive sensing,” in *Proc. IEEE ChinaSIP*, Xi’an, China, Jul. 2014, pp. 232–236.

[27] J. Wang, M. G. Amin, and Y. D. Zhang, “Signal and array processing techniques for RFID readers,” in *Proc. SPIE*, vol. 6248, Orlando, FL, Apr. 2006.

[28] E. Pauls and Y. D. Zhang, “Experimental studies of high-accuracy RFID localization with channel impairments,” in *Proc. SPIE*, vol. 9497, Baltimore, MD, April 2015.

[29] S. Han, H. Lim, and J. Lee, “An efficient localization scheme for a differential-driving mobile robot based on RFID system,” *IEEE Trans. Ind. Electron.*, vol. 54, no. 6, pp. 3362–3369, Dec. 2007.

[30] S. Park and S. Hashimoto, “Autonomous mobile robot navigation using passive RFID in indoor environment,” *IEEE Trans. Ind. Electron.*, vol. 56, no. 7, pp. 2366–2373, Jul. 2009.

[31] S. Park and H. Lee, “Self-recognition of vehicle position using UHF passive RFID tags,” *IEEE Trans. Ind. Electron.*, vol. 60, no. 1, pp. 226–234, Jan. 2013.

[32] B. S. Choi, J. W. Lee, and J. J. Lee, “Localization and map-building of mobile robot based on RFID sensor fusion system,” in *Proc. IEEE Int. Ind. Inform.*, Daejeon, Korea, Jul. 2008, pp. 412–417.

[33] H. J. Lee and H. J. Lee, “Localization of mobile robot based on radio

frequency identification devices," in *Proc. SICE-ICASE*, Busan, Korea, Oct. 2006, pp. 5934–5939.

[34] P. Asadzadeh, L. Kulik, and E. Tanin, "Gesture recognition using RFID technology," *Personal Ubiquitous Comput.*, vol. 16, no. 3, pp. 225–234, Mar. 2012.

[35] D. M. Dobkin, *The RF in RFID: Passive UHF RFID in Practice*, Burlington, MA: Newnes, 2008.

[36] H. Naseri and V. Koivunen,"Indoor mapping based on time delay estimation in wireless networks," in *Proc. IEEE ICASSP*, Brisbane, Australia, Apr. 2015, pp. 2424–2428.

[37] T. S. Rappaport, *Wireless Communications: Principles and Practice*, Upper Saddle River, NJ: Prentice Hall PTR, 2002.

[38] Y. Zhao, N. Patwari, P. Agrawal, and M. G. Rabbat, "Directed by directionality: Benefiting from the gain pattern of active RFID badges," *IEEE Trans. Mobile Comput.*, vol. 11, no. 5, pp. 865–877, May 2012.

[39] N. Gordon, B. Ristic, and S. Arulampalam, *Beyond the Kalman Filter: Particle Filters for Tracking Applications*, Boston, MA: Artech House, 2004.

[40] Alien Technology, ALN-9640 Squiggle Inley Datasheet, Feb. 2014. Available at http://www.alientechnology.com/wp-content/uploads/Alien-Technology-Higgs-3-ALN-9640-Squiggle.pdf